

BER Performance of a Uniform Circular Array Versus a Uniform Linear Array in a Mobile Radio Environment

Giann-An Tsai, R. Michael Buehrer, and Brian D. Woerner

Abstract—In this letter, we present a comparison between the bit error rate (BER) performance of a uniform circular array (UCA) and a uniform linear array (ULA) assuming quadrature phase-shift keying (QPSK) and maximal-ratio-combining (MRC) in a mobile radio communication environment. The results are based on analysis, assuming a flat Rayleigh fading channel with omni-directional antennas and considering the azimuthal plane only. The analytical BER is derived as a function of the spatial fading correlation for both types of antenna arrays. Results show that for similar aperture sizes the UCA outperforms the ULA when considering all angles-of-arrival. However, there is considerable variability over central angle-of-arrival (AOA) for low-to-moderate angle spreads. For angles-of-arrival concentrated near the broadside of the linear array, the ULA typically performs as well as or better than the UCA. A truncated Gaussian AOA (AOA) distribution is assumed to model spatial correlation and the numerical results focus on four element arrays.

Index Terms—Angle spread, circular antenna arrays, diversity performance, fading channels, fading correlation, linear antenna arrays, mobile radio, uniform circular array (UCA), uniform linear array (ULA).

I. INTRODUCTION

IN MOBILE radio communications, multipath propagation causes signal strength fluctuation, thereby inducing signal fading and distortion. To mitigate these channel impairments, antenna arrays have been widely used to improve signal quality, thereby increasing system coverage, capacity, and link quality [1]. Among antenna array configurations, the uniform linear array (ULA) is probably the most common form employed in cellular and personal communication system (PCS) systems. Recently, there has been increased interest in using uniform circular arrays (UCAs). Thus, in this paper, we evaluate the performance of the circular antenna array and compare the bit error rate (BER) performance of the ULA and UCA in Rayleigh fading channels using diversity array combining.

II. SYSTEM MODEL

Without loss of generality, we consider a four-element antenna array for both UCA and ULA configurations. Fig. 1 shows assumed geometry for the uniformly spaced UCA and ULA

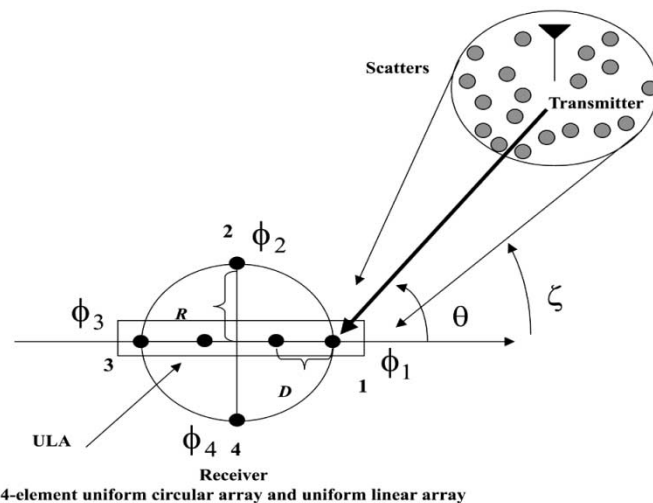


Fig. 1. System model for the four-element UCA and ULA assumed in this letter.

arrays. The ULA consists of four elements located on the x axis while the UCA consists of four elements lying on a circle about the origin. The distance between antennas in the linear array is denoted as D and the radius of the UCA is denoted as R . In the UCA, the angle that each element location makes with the horizontal axis is denoted as ϕ_i . Additionally, it is assumed that the channel is composed of several scatterers which are local to the mobile. Thus, the received signal is the sum of multiple plane waves with random phases, Doppler frequencies and angles-of-arrival based on the position of the scatterers. Each scatterer is associated with an incoming plane wave with an angle-of-arrival (AOA) ζ . The central AOA corresponds to the angular location of the transmitter and is denoted as θ . Following the notation and definitions used in [4], the array manifold vector $\mathbf{v}(\zeta)$ corresponding to each incoming plane wave for a uniform circular array can be written as

$$\mathbf{v}(\zeta) = \begin{bmatrix} v_1(\zeta) \\ v_2(\zeta) \\ \vdots \\ v_M(\zeta) \end{bmatrix} = \begin{bmatrix} e^{-j2\pi \frac{R}{\lambda} \sin(\zeta) \cos(\zeta - \phi_1)} \\ e^{-j2\pi \frac{R}{\lambda} \sin(\zeta) \cos(\zeta - \phi_2)} \\ \vdots \\ e^{-j2\pi \frac{R}{\lambda} \sin(\zeta) \cos(\zeta - \phi_M)} \end{bmatrix} \quad (1)$$

where R is the circular radius of the antenna array, ζ is the elevation AOA, λ is the wavelength of the center frequency of interest, and ζ is the azimuthal AOA. For simplicity, only azimuth angles are considered in the propagation geometry (i.e., $\zeta = 90^\circ$), but the results can be generalized to three dimensions. M is the number of antenna elements, and ϕ_m is the angle of m th element in azimuth plane. For uniform linear arrays, the

Manuscript received February 15, 2002; revised December 24, 2002; accepted February 18, 2003. The editor coordinating the review of this paper and approving it for publication is R. Murch. This work was supported by the MPRG Industrial Affiliates Foundation and by the Defense Advanced Research Projects Agency (DARPA).

The authors are with Mobile and Portable Radio Research Group (MPRG), Virginia Polytechnic Institute, Blacksburg, VA 24073 USA (e-mail: buerher@vt.edu).

Digital Object Identifier 10.1109/TWC.2004.826332

array response vector $\mathbf{v}(\zeta)$ for each incoming plane wave can be written as

$$\mathbf{v}(\zeta) = \begin{bmatrix} v_1(\zeta) \\ v_2(\zeta) \\ \vdots \\ v_M(\zeta) \end{bmatrix} = \begin{bmatrix} 1 \\ e^{-j2\pi \frac{D}{\lambda} \sin(\pi/2-\zeta)} \\ e^{-j2\pi \frac{2D}{\lambda} \sin(\pi/2-\zeta)} \\ \vdots \\ e^{-j2\pi \frac{(M-1)D}{\lambda} \sin(\pi/2-\zeta)} \end{bmatrix} \quad (2)$$

where D is the antenna spacing. Note that $R = 1.5D$ for the assumed four-element UCA-ULA antenna configurations, as shown in Fig. 1.

The time-varying impulse response $\mathbf{h}(t)$ of the flat fading channel is modeled using a vectorized version of Jakes' model [1], [3] and can be expressed as

$$\mathbf{h}(t) = \frac{1}{\sqrt{L}} \sum_{s=1}^L e^{j[2\pi F_d \cos(\Psi_s)t + \Phi_s]} \mathbf{v}(\zeta_s) \quad (3)$$

where L is the number of scatterers used in the Jakes model, Φ_s is a uniformly distributed random phase over $[0, 2\pi]$, Ψ_s is the random angle-of-departure at the mobile relative to the motion of the mobile also assumed uniformly distributed on $[0, 2\pi]$, F_d is the maximum Doppler frequency due to mobility, $\mathbf{v}(\zeta_s)$ is the array response vector defined above for the UCA and ULA, and ζ_s represents the AOA at the base station for the s th scattered path. Note that bold face is used to indicate vectors and matrices. Based on limited field measurement data, the distribution of the AOA at the received base station antenna array is assumed to be a truncated Gaussian AOA distribution which is expressed as

$$f(\zeta_s) = \frac{C_g}{\sqrt{2\pi}\sigma_a} e^{-\frac{(\zeta_s - \theta)^2}{2\sigma_a^2}}, \quad -\pi + \theta \leq \zeta_s \leq \pi + \theta \quad (4)$$

where σ_a is the standard deviation of the corresponding untruncated Gaussian distribution, θ is the central AOA, and C_g is a normalizing constant chosen to make $f(\zeta_s)$ a density function and can be shown to be

$$C_g = \frac{1}{\text{erf}\left(\frac{\pi}{\sqrt{2}\sigma_a}\right)} \quad (5)$$

where $\text{erf}(x)$ is the error function and is defined as

$$\text{erf}(x) = \frac{2}{\sqrt{\pi}} \int_0^x e^{-t^2} dt. \quad (6)$$

Note that this model results in a Rayleigh fading amplitude with uniformly distributed phase at each antenna. Also, the scatterers are assumed to be uniformly distributed about the mobile (i.e., Ψ_s is uniformly distributed on $[0, 2\pi]$) which leads to a standard Doppler spectrum and temporal correlation function [1]. Since we are interested in the effect of angle spread σ_a on the BER performance rather than the effect of Doppler spread on the tracking performance, the channel vector $\mathbf{h}(t)$ is assumed to be quasi-stationary during the i th epoch (i.e., $(1/F_d) \gg T_s$). Note that for this work, we used a value of $L = 50$. This vector channel model is analogous to the one presented in [2] with the exception that here we consider a truncated Gaussian distribution for AOA as opposed to a uniform distribution.

The received signal after matched filtering is sampled at the symbol rate $(1/T_s)$ at each antenna element. The baseband equivalent received signal during the i th symbol at the base station can be expressed as an M -element vector

$$\mathbf{x}[i] = \sqrt{P_r} \mathbf{h}[i] d[i] + \mathbf{n}[i], \quad (7)$$

where $d[i]$ is a quadrature phase-shift keying (QPSK) modulated symbol at the i th symbol epoch, P_r is the average received power at each antenna, $\mathbf{n}[i]$ is additive white Gaussian noise with covariance matrix $\sigma^2 \mathbf{I}_M$, and $\mathbf{h}[i]$ is the discrete vector channel resulting from filtering and sampling $\mathbf{h}(t)$ at the symbol rate. The decision metric for QPSK using maximal-ratio-combining (MRC) combining is well known to be

$$y[i] = \mathbf{w}[i]^\dagger \mathbf{x}[i], \quad (8)$$

where $\mathbf{w}[i]$ is the vector of complex optimum weights, the superscript \dagger denotes the transpose and conjugate and for MRC combining with perfect channel estimation $\mathbf{w}[i]$ is given by [5]

$$\mathbf{w}[i] = \mathbf{h}[i]. \quad (9)$$

III. PERFORMANCE ANALYSIS

Since the BER of QPSK with gray coding is the same as the BER of BPSK, we only need to consider the in-phase component of the decision statistics. The signal components of $y[i]$ can be treated as M complex jointly Gaussian random variables that are a function of the spatial correlation matrix [6]. It is well known [7] that the BER of M -element MRC antenna combining for BPSK can be expressed as function of the eigenvalues of the spatial correlation matrix. That is

$$P_e = \frac{1}{2} \sum_{m=1}^M \frac{\lambda_m^{M-1}}{\prod_{k \neq m} (\lambda_m - \lambda_k)} \left(1 - \sqrt{\frac{\lambda_m}{1 + \lambda_m}} \right) \quad (10)$$

where λ_m are the eigenvalues of the spatial correlation matrix \mathbf{R}_h , which can be defined as

$$\begin{aligned} \mathbf{R}_h &= E \left\{ \frac{P_r}{\sigma^2} \mathbf{h}(t) \mathbf{h}(t)^\dagger \right\} \\ &= \gamma_c \mathbf{R}_v \end{aligned} \quad (11)$$

where γ_c is the received signal-to-noise ratio per bit, per antenna and \mathbf{R}_v is defined as

$$\mathbf{R}_v = E \{ \mathbf{v}(\zeta) \mathbf{v}(\zeta)^\dagger \}. \quad (12)$$

The spatial correlation between the channels seen at the m th and n th antenna elements can then be expressed as

$$\begin{aligned} \mathbf{R}_v(m, n) &= E \{ v_m(\zeta) v_n(\zeta)^* \} \\ &= \int_{\zeta} v_m(\zeta) v_n(\zeta)^* f(\zeta) d\zeta \end{aligned} \quad (13)$$

where $f(\zeta)$ is the probability density function of the AOA. In Appendix A, it is shown that for a truncated Gaussian AOA distribution, the real and imaginary parts of $\mathbf{R}_v(m, n)$ for UCA are given as (see (14) and (15) at the bottom of the following page) where Z_c and α are functions of R, λ , and ϕ_m as shown in Appendix A and $J_n(x)$ is an n th order Bessel function of the first kind.

In Appendix B, it is shown that the real and imaginary parts of $\mathbf{R}_v(m, n)$ for ULA are (see (16) and (17) at the bottom of the following page) where $Z_l = 2\pi((m-n)D)/\lambda$. Thus, for a given configuration, we can calculate the spatial correlation matrix \mathbf{R}_h using (14)–(17). Using the eigenvalues of \mathbf{R}_h , the performance can then be calculated using (10).

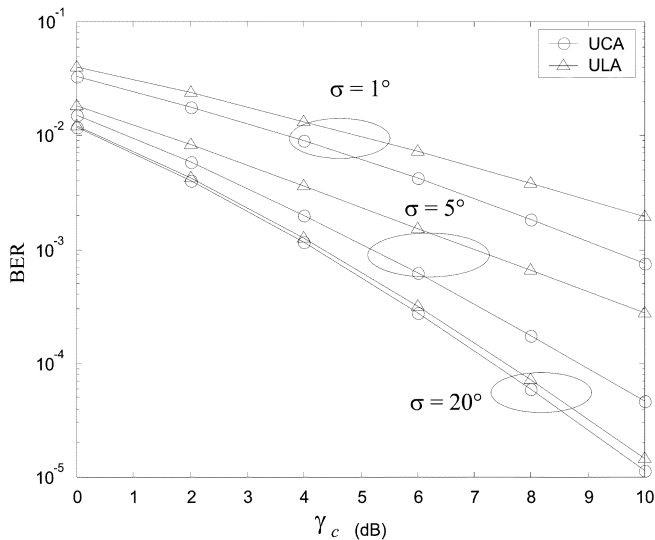


Fig. 2. Analytical BER performance of UCA and ULA for various angle spread variance σ_a with a radius of $R = 5\lambda$ ($D = (10/3)\lambda$). Note that performance is averaged over all values of θ on $[0, 2\pi]$.

IV. RESULTS

Fig. 2 shows the analytical BER performance of the UCA and ULA versus the channel SNR for various values of angle spread, σ_a , with $R = 5\lambda$ and averaged over all values of θ . Note that for a four-element linear array, the element spacing is $D = (2/3)R$, while for the UCA, the minimum spacing between elements is $\sqrt{2}R$. As the angle spread σ_a increases, the spatial fading correlation decreases, thus, the BER performance improves. It is also seen that the UCA outperforms the ULA on average for small and moderate values of σ_a . The performance is nearly identical for large angle spread, since all elements are nearly uncorrelated. At small values of angle spread, there is little diversity advantage for either array, and thus they perform similarly. However, for moderate values of angle spread, the minimum distance advantage of the UCA is seen. For verification purposes, simulations were carried out and compared to the analytical BER results

and they were found to agree. While the results in Fig. 2 provide a fair comparison in terms of equal total array size, they are not equal in terms of the minimum distance between elements. Clearly, for the geometry given in Fig. 1, the minimum distance between elements for the ULA will be smaller than the UCA. One might ask how the performances compare for equal minimum distance. This scenario is plotted in Fig. 3 where $D = (10/3)\lambda$ for the ULA while $R = (10/3\sqrt{2})\lambda$ for the UCA. This provides for equivalent minimum distances, although the linear array will now be larger than the UCA. Here, we see that the performances are nearly identical, although the ULA has a slight advantage in small and moderate angle spreads. Again, the performance is averaged over all values of θ . We should emphasize that the linear extent of the ULA is larger than the linear extent of the UCA.

Fig. 4 shows the performance of the UCA and the ULA as function of θ (AOA) for $R = 5\lambda$, $\gamma_c = 8$ dB and the relative geometry given in Fig. 1. As shown, the UCA significantly outperforms the ULA at endfire ($\theta = 0^\circ$). However, at central AOA values larger than approximately 35° (i.e., as we approach the broadside of the ULA), the linear array performs similarly to or even better than the UCA. The variability in the performance of both arrays is more pronounced at moderate angle spreads ($\sigma_a = 5^\circ$) where the UCA outperforms the ULA by over an order of magnitude at endfire while the ULA provides an order of magnitude improvement over the UCA at $\theta = 45^\circ$. This variability in the ULA performance is due to the fact that the correlation between elements is high for the ULA when the central AOA is near endfire, unless angle spread is very large. The worst case for the UCA is $\theta = 45^\circ$ since in that case elements three and four are directly behind (and, thus, strongly correlated with) elements one and two, as can be seen in Fig. 1. This variation in correlation has been previously reported in [1] and [2].

Fig. 5 plots the performance of both arrays for $\sigma = 1^\circ$ and $\gamma_c = 8$ dB as the antenna spacing increases for different values of θ . Again, the performance of the ULA is poor for $\theta = 0^\circ$ since the correlation across the array is high and, thus, there is little diversity advantage. Increasing the size of the array makes

$$\text{Re}\{\mathbf{R}_v(m, n)\} = \sqrt{(2\pi)} \cdot C_g \cdot \sigma_a \cdot J_0(Z_c) + 2\sqrt{2\pi} C_g \sigma_a \sum_{k=1}^{\infty} e^{-2\sigma_a^2 k^2} J_{2k}(Z_c) \cos(2k(\theta + \alpha)) \quad (14)$$

$$\text{Im}\{\mathbf{R}_v(m, n)\} = 2\sqrt{2\pi} C_g \sigma_a \sum_{k=0}^{\infty} e^{-\frac{(2k+1)^2 \sigma_a^2}{2}} J_{2k+1}(Z_c) \cdot \sin[(2k+1)(\theta + \alpha)] \quad (15)$$

$$\text{Re}\{\mathbf{R}_v(m, n)\} = \sqrt{(2\pi)} \cdot C_g \cdot \sigma_a \cdot J_0(Z_l) + 2\sqrt{2\pi} C_g \sigma_a \sum_{k=1}^{\infty} e^{-2\sigma_a^2 k^2} J_{2k}(Z_l) \cos(2k(\theta)) \quad (16)$$

$$\text{Im}\{\mathbf{R}_v(m, n)\} = 2\sqrt{2\pi} C_g \sigma_a \sum_{k=0}^{\infty} e^{-\frac{(2k+1)^2 \sigma_a^2}{2}} J_{2k+1}(Z_l) \cdot \sin[(2k+1)(\theta)] \quad (17)$$

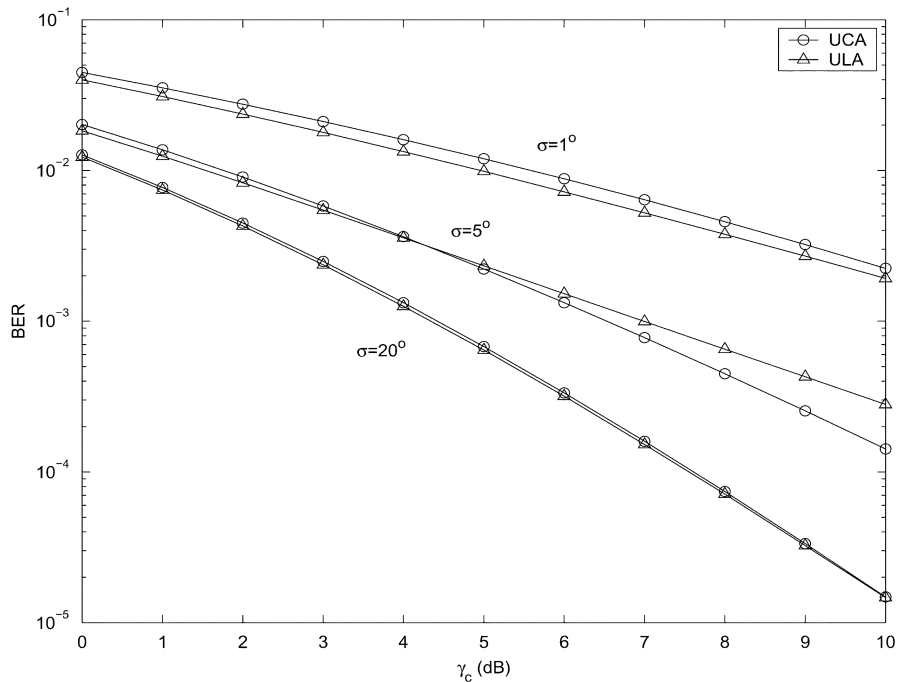


Fig. 3. Analytical BER performance of UCA and ULA for various angle spread variance σ_a with common minimum distance between elements (For UCA $R = (10/3\sqrt{2})\lambda$ while for ULA $D = (10/3)\lambda$). Note that performance is averaged over all values of θ on $[0, 2\pi]$.

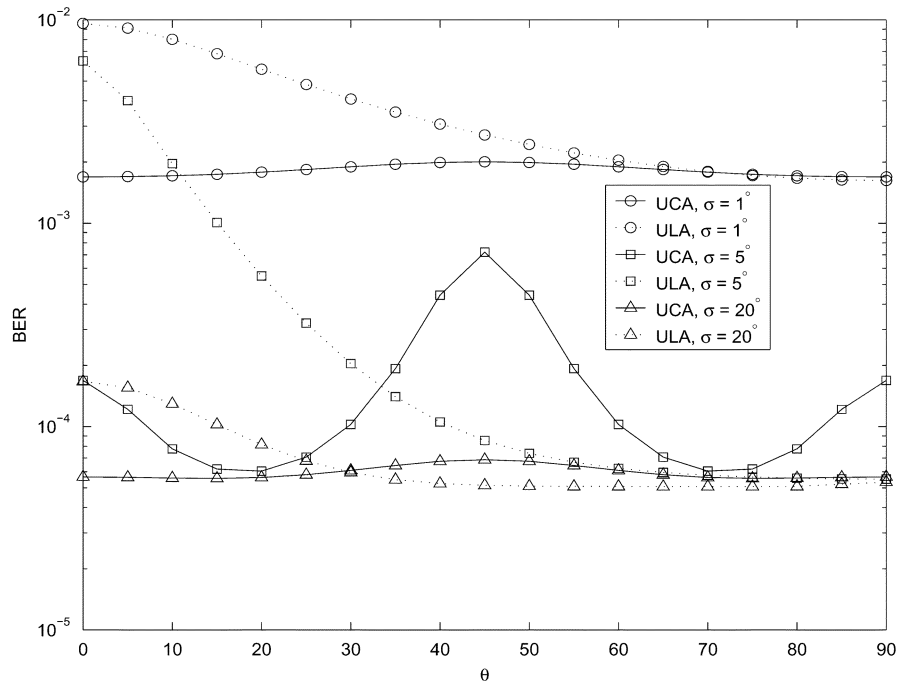


Fig. 4. Analytical BER performance of UCA and ULA as function of central AOA θ for various angle spreads ($\gamma_C = 8$ dB, $R = 5\lambda$).

little difference in this case, as can be seen.¹ Note that as R is increased, the relative geometry given in Fig. 1 is held constant. As the array size increases, we see performance floors as is expected. Interestingly, however, the error floors are not equal. One might expect that all cases would approach the performance of four branch diversity performance ($P_e = 5 * 10^{-5}$ in this

¹If the fading rate were significantly faster, increasing the array size would make more difference in the ULA case.

case) as R increases. However, we have already noted that we do not see this behavior for the ULA at $\theta = 0$. Again this is because all four elements are inline with the central AOA leading to high correlation between elements. However, for other values of θ , the ULA does approach the four-branch diversity performance since the four elements eventually become uncorrelated. The UCA also shows improving performance for $\theta = 0^\circ, 45^\circ, 80^\circ$ with increasing R but shows error floors at different BER values. As expected, the worst case is $\theta = 45^\circ$. Again, in

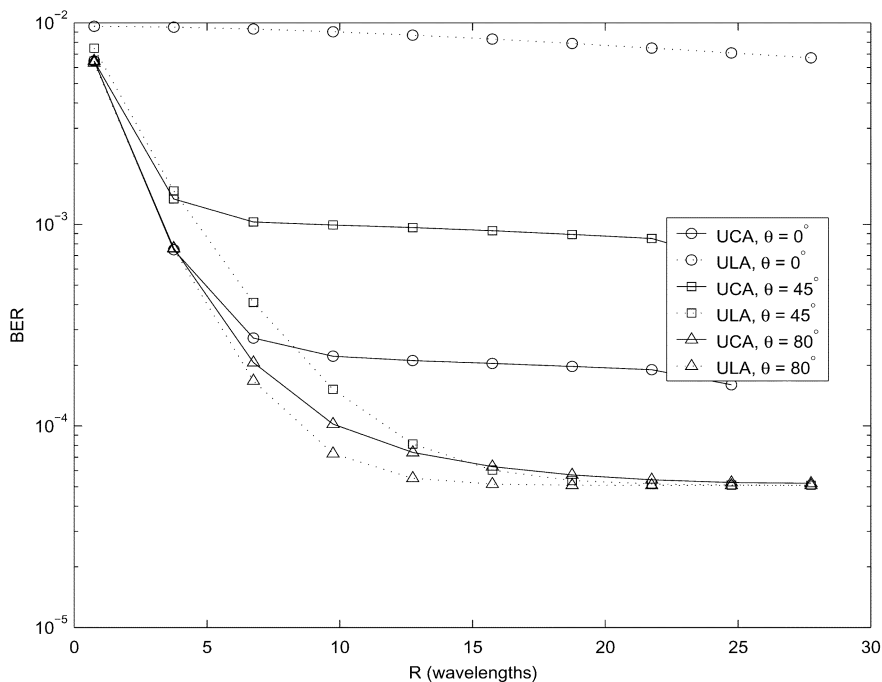


Fig. 5. Analytical BER performance of UCA and ULA for various central angles-of-arrival ($\gamma_C = 8$ dB, $\sigma_a = 1^\circ$).

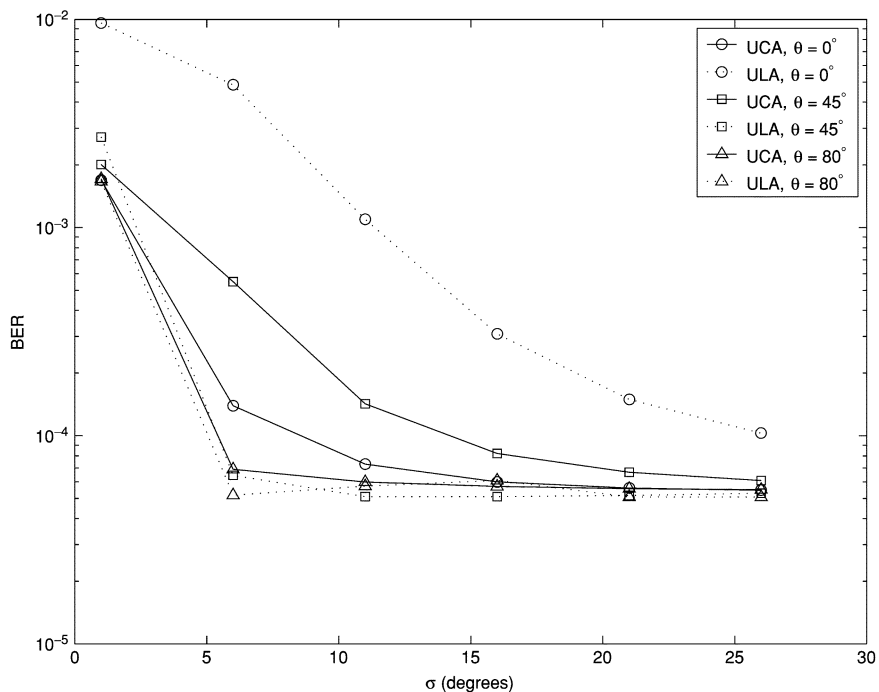


Fig. 6. Analytical BER performance of UCA and ULA for various central angles-of-arrival ($\gamma_C = 8$ dB, $R = 5\lambda$).

this case elements three and four are directly behind elements one and two and, thus, will be highly correlated with those elements even for large values of R . Thus, as R increases the performance approaches the performance of two branch diversity and decreases very slowly afterwards. At $\theta = 0^\circ$, element three is directly behind (and, thus, highly correlated with) element one. Thus, as R increases the performance quickly approaches three-branch diversity performance. At $\theta = 80^\circ$, however, all

four elements become decorrelated as R is increased and, thus, does approach four-branch diversity performance.

Fig. 6 plots the performance of arrays for $R = 10\lambda$ as the angle spread σ increases. Again, the relative geometry is held constant. We note that in this case all curves approach the performance of four branch diversity as σ_a increases. For large σ_a , the AOA distribution approaches a uniform distribution which will provide low correlation among antennas for any value of θ .

V. CONCLUSION

In this letter, we compare the diversity performance of a uniform circular array and a uniform linear array using maximal ratio combining in a mobile radio environment. Diversity performance is evaluated based on BER results. The analytical BER is derived as function of antenna correlation for both types of antenna arrays. Results show that the UCA outperforms the ULA **on average** for small and moderate angle spread for similar aperture sizes. However, the ULA outperforms the UCA for certain angles-of-arrival (e.g., near broadside of the ULA) with moderate angle spreads. All other conditions resulted in similar performance between the arrays. With small values of angle spread, there is little diversity advantage from either array, while for large angle spreads both arrays provide four-branch diversity performance. Results also show that the central AOA can have a significant impact on the BER performance of both the UCA and the ULA.

APPENDIX A

Using the definition of (13), the array spatial correlation between the m th and n th antenna elements for a truncated Gaussian AOA distribution can be expressed as

$$\begin{aligned} \mathbf{R}_v(m, n) &= \int_{\zeta} v_m(\zeta) v_n(\zeta)^* f(\zeta) d\zeta \\ &= \int_{-\pi+\theta}^{\pi+\theta} e^{-j2\pi \frac{R}{\lambda} \{[\cos \phi_m - \cos \phi_n] \cos(\zeta) + [\sin \phi_m - \sin \phi_n] \sin(\zeta)\}} \\ &\quad \times C_g e^{-\frac{(\zeta-\theta)^2}{2\sigma_a^2}} d\zeta. \end{aligned} \quad (18)$$

Let

$$K_1 = 2\pi \frac{R}{\lambda} [\cos(\phi_m) - \cos(\phi_n)] \quad (19)$$

$$K_2 = 2\pi \frac{R}{\lambda} [\sin(\phi_m) - \sin(\phi_n)]. \quad (20)$$

Using the definitions of (19) and (20), we can rewrite (18) as

$$\mathbf{R}_v(m, n) = C_g \int_{-\pi+\theta}^{\pi+\theta} e^{-j(K_1 \cos(\zeta) + K_2 \sin(\zeta))} e^{-\frac{(\zeta-\theta)^2}{2\sigma_a^2}} d\zeta. \quad (21)$$

Let

$$\sin(\alpha) = \frac{K_1}{\sqrt{K_1^2 + K_2^2}} \quad (22)$$

$$\cos(\alpha) = \frac{K_2}{\sqrt{K_1^2 + K_2^2}} \quad (23)$$

$$Z_c = \sqrt{K_1^2 + K_2^2}. \quad (24)$$

Using the definitions of (22)–(24), we can rewrite (21) as

$$\mathbf{R}_v(m, n) = C_g \int_{-\pi+\theta}^{\pi+\theta} e^{-jZ_c \{\sin(\alpha+\zeta)\}} e^{-\frac{(\zeta-\theta)^2}{2\sigma_a^2}} d\zeta. \quad (25)$$

Letting $x = \zeta - \theta$, we can rewrite the real and imaginary parts of (25) as follows:

$$\text{Re}\{\mathbf{R}_v(m, n)\} = C_g \int_{-\pi}^{\pi} \cos[Z_c \sin(\alpha + \theta + x)] e^{-\frac{x^2}{2\sigma_a^2}} dx \quad (26)$$

$$\text{Im}\{\mathbf{R}_v(m, n)\} = C_g \int_{-\pi}^{\pi} \sin[Z_c \sin(\alpha + \theta + x)] e^{-\frac{x^2}{2\sigma_a^2}} dx. \quad (27)$$

By making use of the well-known of a series expansion, $\cos[Z_c \sin(\varphi)]$ and $\sin[Z_c \sin(\varphi)]$ can be further represented as, respectively,

$$\cos[Z_c \sin(\varphi)] = J_0(Z_c) + 2 \sum_{k=1}^{\infty} J_{2k}(Z_c) \cos(2k\varphi) \quad (28)$$

$$\sin[Z_c \sin(\varphi)] = 2 \sum_{k=0}^{\infty} J_{2k+1}(Z_c) \sin((2k+1)\varphi). \quad (29)$$

By integrating (26) and (27) with the substitution of (28) and (29), respectively, we can obtain (14) and (15).

APPENDIX B

Using the definition of (13), the array spatial correlation between the m th and n th antenna elements for a truncated Gaussian AOA distribution can be expressed as

$$\begin{aligned} \mathbf{R}_v(m, n) &= \int_{\zeta} v_m(\zeta) v_n(\zeta)^* f(\zeta) d\zeta \\ &= \int_{-\pi+\theta}^{\pi+\theta} C_g e^{-jZ_l \sin(\zeta)} e^{-\frac{(\zeta-\theta)^2}{2\sigma_a^2}} d\zeta \end{aligned} \quad (30)$$

where $Z_l = 2\pi((m-n)D)/\lambda$. Letting $x = \zeta - \theta$, we can rewrite the real and imaginary parts of (30) as follows:

$$\text{Re}\{\mathbf{R}_v(m, n)\} = C_g \int_{-\pi}^{\pi} \cos[Z_l \sin(\theta + x)] e^{-\frac{x^2}{2\sigma_a^2}} dx \quad (31)$$

$$\text{Im}\{\mathbf{R}_v(m, n)\} = C_g \int_{-\pi}^{\pi} \sin[Z_l \sin(\theta + x)] e^{-\frac{x^2}{2\sigma_a^2}} dx. \quad (32)$$

By integrating (31) and (32) with the substitution of (28) and (29), respectively, we can obtain (16) and (17).

REFERENCES

- [1] W. C. Jakes, *Microwave Mobile Communications*, 1st ed. New York: Wiley, 1974.
- [2] J. Salz and J. H. Winters, "Effect of fading correlation on adaptive arrays in digital mobile radio,," *IEEE Trans. Veh. Technol.*, vol. 43, pp. 1049–1057, Nov. 1994.
- [3] J.-A. Tsai and B. D. Woerner, "The fading correlation function of a circular antenna array in mobile radio environment,," in *Proc. 54th GLOBECOM*, vol. 3, Nov. 2001, pp. 1630–1634.
- [4] W. L. Stutzman and G. A. Thiele, *Antenna Theory and Design*, 1st ed. New York: Wiley, 1981.
- [5] J. G. Proakis, *Digital Communications*, 3rd ed. New York: McGraw-Hill, 1995.
- [6] D. Brennan, "Linear diversity combining techniques,," in *Proc. IRE*, vol. 47, 1959, pp. 1075–1102.
- [7] M. Schwartz, W. Bennett, and S. Stein, *Communication Systems and Techniques*. New York: McGraw-Hill, 1966.